










Comparative homology of *Pleurotus ostreatus* laccase enzyme: Swiss model or Modeller?

Marco Antonio Silva^a , José Cordeiro do Nascimento Júnior^b , Douglas Vieira Thomaz^c , Rafael Trindade Maia^e , Vinícius Costa Amador^f , Giovana Tommaso^a  and Glauciane Danusa Coelho^d 

^aLaboratory of Environmental Biotechnology, Faculty of Animal Science and Food Engineering, University of São Paulo, Pirassununga, São Paulo, Brazil; ^bCenter for Water Resources and Environmental Studies, São Carlos School of Engineering, University of São Paulo, São Carlos, São Paulo, Brazil; ^cNational Enterprise for nanoScience and nanoTechnology (NEST), Istituto Nanoscienze-CNR and Scuola Normale Superiore, Pisa, Italy; ^dAcademic Unit of Biotechnology Engineering; Center for Sustainable Development of the Semi-Arid, Federal University of Campina Grande, Sumé, Paraíba, Brazil; ^eAcademic Unit of Rural Education; Center for Sustainable Development of the Semi-Arid, Federal University of Campina Grande, Sumé, Paraíba, Brazil; ^fBioscience Center, Genetics Department, Federal University of Pernambuco, Recife, Brazil

Communicated by Ramaswamy H. Sarma

ABSTRACT

Laccases stand out in the industrial context due to their versatile biotechnological applications. Although these enzymes are frequently investigated, currently, *Pleurotus ostreatus* laccase structural model is unknown. Therefore, this research aims to predict and validate a *P. ostreatus* laccase theoretical model by means of comparative homology. The laccase target's primary structure (AOM73725.1) was obtained from the NCBI database, the model was predicted from homologous structures obtained from the PDB (PDB-ID: 5A7E, 2HRG, 4JHU, 1GYC) using the Swiss-Model and Modeller, and was refined in GalaxyRefine. The models were validated using PROCHECK, VERIFY 3D, ERRAT, PROVE and QMEAN Z-score servers. Moreover, molecular docking between the laccase model (Lacc4MN) and ABTS was performed on AutoDock Vina. The models that were generated by the Modeller showed superior stereochemical and structural characteristics to those predicted by the Swiss Model. The refinement made it difficult to stabilize the copper atoms which are typical of laccases. The Lacc4MN model showed the interactions between the amino acids in the active site of the laccase and the copper atoms, thereby hinting the stabilization of the metal through electrostatic interactions with histidine and cysteine. The molecular docking between Lacc4MN and ABTS showed negative free energy and the formation of two hydrogen bonds involving the amino acids ASP 208 and GLY 268, and a Pi-sulfur bond between residue HIS 458 and ABTS, which demonstrates the typical catalytic functionality of laccases. Furthermore, the theoretical model Lacc4MN presented stereochemical and structural characteristics that allow its use *in silico* tests.

ARTICLE HISTORY

Received 15 July 2022
Accepted 17 October 2022

KEYWORDS

ABTS; basidiomycete;
ligninolytic enzyme;
molecular docking; *in silico*

Introduction


Laccases are multicopper oxidases with three to four copper atoms that are distributed between three bonding sites (Daronch et al., 2020; Singh & Gupta, 2020). These sites are divided into Type 1 (Cu T1), Type 2 (Cu T2) and Type 3 (Cu T3a and Cu T3b). The Cu T1 (blue copper) imparts the typical blue color to the protein and catalyzes the transfer of electrons from the substrate to the Cu T2 and Cu T3 sites (electron acceptors), where molecular oxygen is reduced to water (Leonowicz et al., 2001; Ren & Yuan, 2015).

The investigation of fungal laccases in biotechnological applications has been crescent over the years, and there is a rich literature concerning this field of research (Ardila-Leal et al., 2021; Leynaud Kieffer Curran et al., 2022; Khatami et al., 2022; Martínková et al., 2022; Rostami et al., 2022; Villalba-Rodríguez et al., 2022), from their noteworthy

potential in the remediation of effluents that are contaminated with residues of lignocellulosic, textile, aromatic, phenolic and herbicide nature (Kumar & Sharma, 2017; Ballaminut et al., 2019; Mäkelä et al., 2020; Coelho et al., 2020).

The fungal enzyme appliance for effluent treatment allows the straightforward removal of recalcitrant chemical compounds by promoting their structural degradation or mineralization. Among these fungal enzymes, laccases stand out, which are unspecific (EC 1.10.3.2, p-diphenol: dioxygen oxidoreductase) belonging to the multidomain cupredoxin family, and they are also synthesized by plants, fungi and bacteria (Bertrand et al., 2002; Maestre-Reyna et al., 2015; Arregui et al. 2019). In addition, the application of laccase covers the production of cellulosic ethanol and the development of biosensors, as well as a variety of technologies in the food and pharmaceutical industry (Bezerra et al., 2015;

CONTACT Glauciane Danusa Coelho  glauciane.coelho.pb@gmail.com, glauciane.danusa@professor.ufcg.edu.br  Academic Unit of Biotechnology Engineering; Center for Sustainable Development of the Semi-Arid, Federal University of Campina Grande, Sumé, Paraíba, Brazil.

 Supplemental data for this article can be accessed online at <https://doi.org/10.1080/07391102.2022.2138975>

© 2022 Informa UK Limited, trading as Taylor & Francis Group

Brugnerotto et al., 2017; Zerva et al., 2019; Masjoudi et al., 2021).

Despite the biotechnological importance of laccases, and the well-reported use of *Pleurotus ostreatus* for several applications, no three-dimensional model for *P. ostreatus* laccases were proposed previously. In this regard, the emerging interest of the biotechnology industry in environmental sustainability strategies development that follows the urgent needs. In this sense, several authors highlight that *in silico* prediction approach as a direct screening research could reduce experimental costs. To all accounts, computational methods have extensively contributed to the elucidation of the three-dimensional structures of proteins and bypassed the limitations of experimental methods such as insufficient material for analysis, inefficiency in crystallization, high cost and operating time (Chou, 2004; Kaur et al., 2019).

Amongst these techniques, homology modeling stands out as a valuable approach, which allows the prediction and understanding of the ultrastructural features of proteins, while concomitantly providing data for the prediction of their biochemical characteristics and evolutionary changes (Koonin & Galperin, 2003; Awasthi et al., 2015). In this type of modeling, the three-dimensional structure of a given protein is predicted from the amino acid sequence, based mainly on its alignment with one or more proteins of known three-dimensional structure. There are several servers/software available for determining protein structures, as described by Bongirwar and Mokhade (2022). In this research, we used the Swiss Model server, which was the first fully automated protein homology modeling server (Waterhouse et al., 2018), and the MODELLER package, which also automatically calculates a model containing all non-hydrogen atoms, satisfying the spatial constraints, but which requires users to use a programming command (Šali & Blundell, 1993; Fiser et al., 2000). Furthermore, computational modeling also allows the proposition of binding mechanisms to small ligands and the modeled proteins, which has been extensively proven as a viable alternative to *in vivo* and *in vitro* testing (Thakuria et al., 2015).

Therefore, owing to the relevance of *P. ostreatus* in biotechnology, and the lack of models for the ligninolytic enzyme produced by this fungus; this research aimed to develop and validate a theoretical model of *P. ostreatus* laccase using the comparative homology approach. In order to achieve this objective, the Modeller program and the Swiss model server were evaluated. In addition, the possibility of metalloprotein refinement was analyzed to improve the stereochemical characteristics of the model. The model that showed the best stereochemical characteristics was validated by several standard methods, including the position of copper atoms.

Methodology

Identification of homologous structures

The primary structure of the *Pleurotus ostreatus* laccase (GenBank: AOM73725.1) was obtained from the NCBI (National Center for Biotechnology Information) database.

The target sequence was aligned in the BLASTp program (<https://blast.ncbi.nlm.nih.gov/Blast.cgi>) with the template's primary structure from PDB (Protein Data Bank) (Altschul et al., 1997). The ten homologous models that presented the highest Max score in BLASTp were evaluated, and from the analysis of the Query coverage, e-value, amino acid identity, resolution of the template protein and the R-factor (R-value free) the best models were selected to be used as a template.

Primary structure analysis

The AOM73725.1 primary structure and ten best-retrieved outputs in the last step had their primary structure analyzed with multiple alignments. The comparison of conserved regions between the primary structures was performed using multiple alignment software Bioedit (v.7.2) (<https://bioedit.software.informer.com/7.2/>) and ClustalW algorithm, the gap penalty was kept as default parameters (Thompson et al., 1994) was used. The amino acid sequence analysis of *P. ostreatus* laccase was performed to identify the presence of conserved domains and was predicted by InterProScan algorithm (<https://www.ebi.ac.uk/interpro/search/sequence/>) (Zdobnov & Apweiler, 2001).

P. ostreatus laccase modelling

The Swiss-model server (<https://swissmodel.expasy.org/interactive>) (Guex & Peitsch, 1997; Bienert et al., 2017; Waterhouse et al., 2018) and the Modeller package (https://salilab.org/modeller/download_installation.html) (Šali & Blundell, 1993) were used to predict the theoretical models of *P. ostreatus* laccase using the homology modeling technique (Martí-Renom et al., 2000; Webb & Sali, 2016). The theoretical laccase models were refined by GalaxyRefine server (Heo et al., 2013).

Theoretical model validation

A multilayer approach was applied in theoretical models for validation. The first the model's stereochemical analysis was made by Ramachandran plot on PROCHECK server (Laskowski et al., 1993).

The second step was based on the compatibility analysis between the protein's three-dimensional structure and its own amino acid sequence in VERIFY 3D, thereby requiring that at least 80% of the amino acids have a score greater than or equal to 0.2 in the 3D/1D profile (Bowie et al., 1991).

The third step was based on the analysis of the relative frequencies of non-covalent interactions between the various types of atoms in the ERRAT. Therefore, in order to a model to be considered of high quality, the overall quality factor values has to be greater than 50 (Colovos & Yeates, 1993; Messaoudi et al., 2013).

The fourth step was based on the comparison between atomic volumes and sets of default values, which were pre-calculated in PROVE with desirable margin on ranges between 0 and 1%, while the warning margin comprises

Table 1. Ten sequences that showed the best Max score values with primary structure AOM73725.1 in the BLASTp program.

Microorganism	GI Number	PDB-ID	Max Score	Identity (%)	Res (Å)	RV
<i>Trametes versicolor</i>	23200086	1GYC	636	64.55%	1.90	0.212
<i>Corioliopsis gallica</i>	350610907	4A2D	623	63.55%	2.30	0.228
<i>Corioliopsis gallica</i>	385251975	4A2F	623	63.55%	1.90	0.224
<i>Corioliopsis gallica</i>	1032208307	5A7E	623	63.15%	1.50	0.183
<i>Corioliopsis trogii</i>	158428663	2HRG	622	62.95%	1.58	0.192
<i>Aspergillus oryzae</i>	1727108819	6H5Y	619	62.95%	2.30	0.203
<i>Corioliopsis caperata</i>	635576677	4JHU	612	63.07%	1.89	0.210
<i>Trametes coccinea</i>	1276810306	5NQ8	612	63.25%	2.00	0.173
<i>Cerrena sp.</i>	1474892261	5Z1X	610	63.67%	1.38	0.149
<i>Trametes sanguinea</i>	1276810305	5NQ7	607	62.79%	2.75	0.207

Caption: GI Number: GenInfo Identifier; PDB-ID: protein identification in the Protein Data Bank; Max Score: highest alignment score (bit-score) between the target sequence and the sequences that are present in the PDB; IDENTITY: percentage of amino acids of the template sequence that are identical to those of the target sequence; RES: model resolution in ångströms; RV: R-Value Free (R-factor). Source: Survey data, 2022.

1–5%. The models with a percentage above 5% are considered inadequate (Pontius et al., 1996). The toolset, including PROCHECK, VERIFY 3D, ERRAT and PROVE, is available on the SAVES v6.0 structural analysis and verification server (<https://saves.mbi.ucla.edu/>).

The fifth step comprised the analysis of the overall structural quality of all models. Models were evaluated through their overall QMEAN score and compared with the experimental structures Z-score (<https://swissmodel.expasy.org/qmean/>). In this score, the values around 0.0 indicate that the structure is "native-like," while scores below -4.0 indicate that the model is of low quality (Benkert et al., 2009).

Structural analysis of theoretical models

The structural analysis of the models was made in PyMOL, version 1.2r3pre, Schrödinger, LLC (<https://pymol.org/2/>). Through this software, the comparison between the positioning of copper atoms and amino acids of the selected refined and unrefined models was carried out. It is worth noting that the position of the copper atoms in the Modeller program was manually adjusted, so that it fits within the allowed distances. Moreover, the comparison of the aforementioned residues with the homologous model was also conducted. The extensive evaluation of the interatomic distances that were observed in the models was computed and their RMSD (Root Mean Squared Deviation) was determined in PyMOL. This parameter is descriptive of the similarity between the structures, being higher values suggestive of higher similarity. Furthermore, the QMEANDisCo (<https://swissmodel.expasy.org/qmean/>) was also used. This parameter has a range of 0 to 1, with scores below 0.6 indicating low model quality (Studer et al., 2020). On the same hand, the analysis of the secondary structures was conducted in the PDBsum (<http://www.ebi.ac.uk/thornton-srv/databases/cgi-bin/pdbsum/GetPage.pl?pdbcode=index.html>) (Laskowski et al., 2018), and the identification of the Cu T1 active site of the laccase structure was performed on the Ghecom server (<https://pdj.org/ghecom/>) (Kawabata & Go, 2007), followed by the prediction of the electrostatic surface of the structure in the APBS-PDB2PQR software (<https://server.poissonboltzmann.org/>).

To this purpose, CHARMM force field (Miyazawa et al., 2017) was used and pH 8.0 was set, as described for the protonation of the *P. ostreatus* laccase model POXA1b (Giacobelli et al., 2017). PyMOL was used to visualize the electrostatic surface, and to compare the amino acids that are part of the active site of the model. The template herein used was an experimentally obtained structure of *Trametes versicolor* laccase (PDB-ID: 1KYA) (Bertrand et al., 2002).

Molecular docking simulation between laccase and ABTS

The .pdb file of the ABTS molecule (2,2'-azino-bis (3-ethyl-benzothiazoline-6-sulfonic acid)) was obtained from the PubChem server (Kim et al., 2021). The preparation of the ligand for the molecular docking simulation was performed using the UCSF Chimera (<https://www.cgl.ucsf.edu/chimera/download.html>) (Pettersen et al., 2004), and the addition of hydrogens was performed using the Dock Prep tool. The volume of the docking grid was $X=14.6736 \text{ \AA}$, $Y=25.613 \text{ \AA}$, $Z=12.9 \text{ \AA}$, and centered at $X=5.04339 \text{ \AA}$, $Y=-44.7222 \text{ \AA}$ and $Z=-23.1315 \text{ \AA}$. The region for the docking study was defined according to the size of the pocket near Cu T1 of the selected model, based on the connection pocket of the 3D structure 1KYA. The number of docking poses that were calculated was of 10, the search exhaustiveness was set to 8, and the maximum energy difference (kcal mol^{-1}) was set to 3. Molecular docking was performed with the AutoDock Vina tool (<https://vina.scripps.edu/downloads/>) (Trott & Olson, 2009), in semi-rigid/semi-flexible mode and the visual analysis of the poses was carried out in Discovery Studio software (<https://discover.3ds.com/discovery-studio-visualizer-download>) (BIOVIA, 2022).

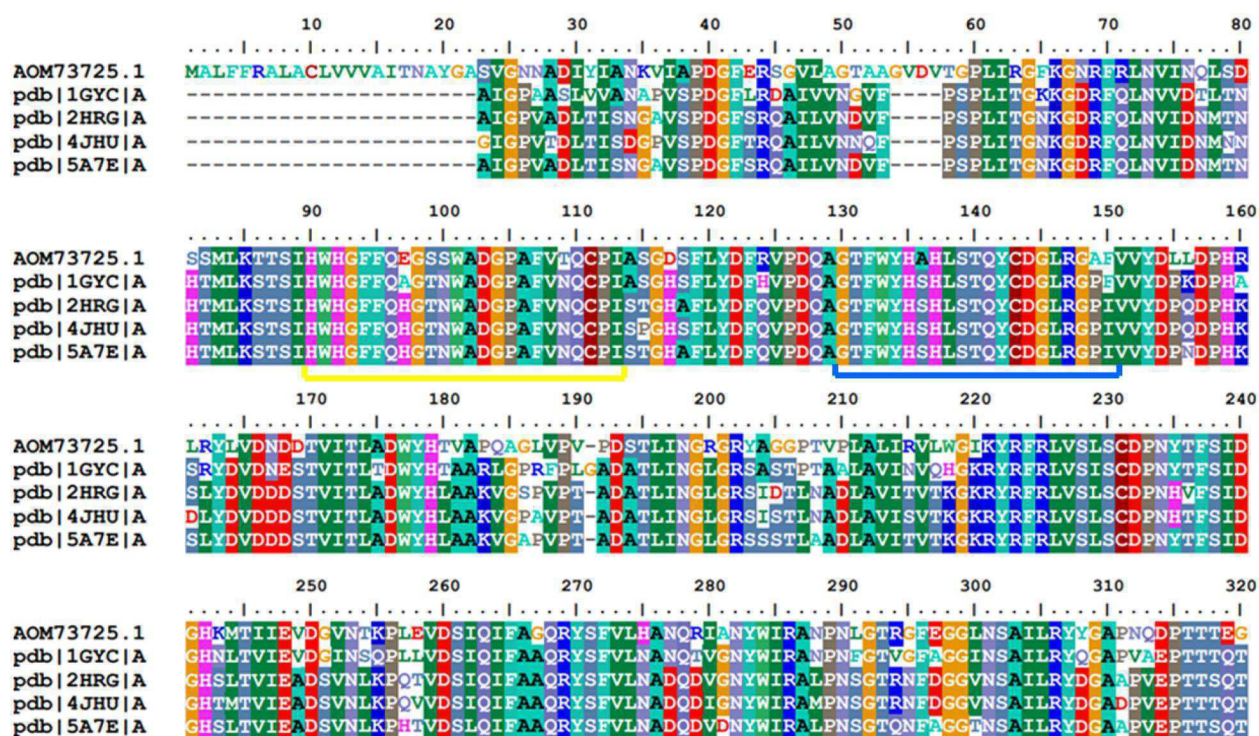
Results and discussion

Identification of homologous structures

The BLASTp retrieved output 59 laccase primary structures of different organisms. Amongst these sequences, the first 10 that presented high Max score values with the target primary structure AOM73725.1 are represented in Table 1 (Figure S1). In addition, these 10 sequences showcased an e-value close to zero and Query coverage (alignment coverage percentage) between 94 and 97%.

An accurate model prediction through homology modeling approach requires at least 30% identity between query and template (Chung & Subbiah, 1996; Jang et al., 2020). Otherwise, when the identity is greater than 50%, there is a drastic reduction in the divergence of functional regions (Fiser, 2017). In this sense, all the structures presented (Table 1) were considered for the prediction of the theoretical model of *P. ostreatus* laccase by the comparative homology method, as they presented highest observed identity, from 62.95 to 64.55% (PDB-ID: 1GYC, 5Z1X, 4A2D and 4A2F).

Additionally, AOM73725.1 has a monomeric structure with 4 copper atoms, including T2 Cu (Palmieri et al., 1997; Hublik & Schinner, 2000; Mansur et al., 2003). In this sense, excelling



Source: Survey data, 2022.

Figure 1. Multiple alignments of primary structure AOM73725.1 with structures 1GYC, 5A7E, 2HRG and 4JHU. The regions underlined and colored in yellow, blue, orange and purple correspond to the conserved regions of the laccases, respectively, L1, L2, L3 and L4. Source: Survey data, 2022.

a high compatible template for the predictable model, the laccase templates like homodimeric structure (PDB-ID: 5Z1X) (Wu et al., 2018) and the absence of Cu T2 (PDB-ID: 4A2D and 4A2F) (De la Mora et al., 2012) were discarded from the modeling approaches.

Furthermore, the allowed identity margin is a considerable choosing criterion for a well-chosen template; this parameter does not consider structural differences (Álvarez-Machancoses et al., 2020). Additionally, other factors, such as structural composition (monomers/dimers) and copper sites, max score, resolution and R-value were considered to choose the possible templates (Ohlendorf, 1994; Šali et al., 1995). In this sense, the R-value free values of templates that were between 0.149 and 0.292 were considerable for a better suitable template to the phylum Basidiomycota, except *Aspergillus oryzae* laccase (PDB-ID: 6H5Y) (de Salas et al., 2016) craving for a reliable theoretical model.

Finally, the structures 5A7E, 2HRG, 4JHU and 1GYC presented low R-values (0.183, 0.192, 0.210 and 0.212), respectively, and showcased resolution values lower than 2 Å (1.50, 1.58, 1.89 and 1.90 Å), respectively. These features denote a good quality of the models (Maia et al., 2021), and for this reason, they were selected as possible templates for the prediction of the theoretical model of *P. ostreatus* laccase.

Multiple alignment

The multiple alignment between the target primary structure AOM73725.1 and the structures 1GYC, 5A7E, 2HRG and 4JHU (Figure 1) showed conserved regions in all evaluated structures that make up the three characteristic domains of the

cupredoxin superfamily (CDD-ID: CL19115) (Piontek et al., 2002; Matera et al., 2008; De la Mora et al., 2012; Glazunova et al., 2015). In addition, four conserved regions were identified, designated as the L1, L2, L3 and L4 regions, within these regions are a total of 10 histidines and 1 cysteine that interact with binding site coppers. These regions are conserved in all multicopper oxidases, and in laccases, these regions are composed of the following amino acids: L1 (H-W-H-G-X9-D-G-X5-QCPI), L2 (G-T-X-W-Y-H-S-H-X3-Q-Y-C-X-D-G-L-X-G-X-(FLIM)), L3 (H-P-X-H-L-H-G-H) and L4 (G-(PA)-W-X-(LFV)-HCHI-DAE-X-H-X3-G-(LMF)-X3-(LFM)), residue X represents an undefined residue, while residues between parentheses represent a partially conserved residue (Kumar et al., 2003).

In the multiple alignment, it is also possible to identify five cysteine residues conserved at positions 111, 143, 231, 481 and 516. In addition, the primary structure AOM73725.1 presented a leftover cysteine (position 10) outside of the conserved domain. Generally, cysteines are conserved among related proteins, and the cysteine connectivity pattern may indicate that the proteins have a similar three-dimensional structure (Thangudu et al., 2008). In this sense, four of these cysteines are protagonists of two structurally conserved disulfide bonds (111-516; 143-231) (Lyashenko, Zhukhlistova, et al. 2006; Lyashenko et al., 2006), except for 5A7E, which showcased only one (143-231). Additionally, according to Fu et al. (2020), in *Amylostereum areolatum* laccases, almost all analyzed sequences contained five cysteine residues and at least one disulfide bridge.

Furthermore, the cupredoxin superfamily fold usually consists of a beta-sandwich with 7 strands in 2 beta-sheets, which is arranged in a Greek-key beta-barrel. The protein

Table 2. Validation of laccase theoretical models predicted by the Swiss-Model server and in the Modeller program, unrefined and refined in GalaxyRefine, through the Ramachandran, 3D VERIFY, ERRAT and PROVE graph.

MODEL	RMF (%)	RAP (%)	RGP (%)	RNP (%)	3D		PROVE (%)
					VERIFY (%)	ERRAT (%)	
Lacc1SN	87.0	11.8	0.7	0.5	97.80	87.5519	3.6
Lacc2SN	88.5	10.6	0.7	0.2	98.00	90.0204	4.7
Lacc3SN	89.4	9.9	0.0	0.7	99.60	87.7339	3.7
Lacc4SN	88.4	10.6	0.2	0.7	98.39	90.2692	3.3
Lacc1MN	91.0	8.0	0.7	0.2	97.58	74.1273	4.9
Lacc2MN	91.1	8.2	0.5	0.2	94.77	72.1881	3.7
Lacc3MN	89.9	9.2	0.7	0.2	97.18	61.8852	5.8*
Lacc4MN	90.1	9.2	0.7	0.0	98.39	66.3265	3.7
Lacc1SR	89.4	9.4	0.2	1.0	99.20	88.6598	4.9
Lacc2SR	90.4	8.9	0.2	0.5	99.20	88.3673	5.3*
Lacc3SR	90.8	8.0	0.5	0.7	98.99	92.3395	4.6
Lacc4SR	90.3	8.5	0.7	0.5	96.57	91.3043	4.1
Lacc1MR	92.0	7.3	0.5	0.2	94.34	81.9127	5.2*
Lacc2MR	92.3	7.0	0.2	0.5	96.98	84.5361	5.2*
Lacc3MR	91.3	7.7	0.7	0.2	99.19	84.1237	4.9
Lacc4MR	91.1	8.0	0.5	0.5	99.80	84.8980	5.1*

Legend: Each model was identified by an alphanumeric set, Lacc represents laccase, the fourth character represents the template structure (1 - 1GYC; 2 - 5A7E; 3 - 2HRG; 4 - 4JHU), fifth character represents the method by which the model was predicted (S - Swiss-Model; M - Modeller), the sixth character indicates whether the structure has been refined (R) or not (N). RMF: percentage of loss in the most favorable regions [A, B, L]; RAP: percentage of residues in additional allowed regions [a, b, l, p]; RGP: percentage of residues in generously allowed regions [~a, ~b, ~l, ~p]; RNP: percentage of loss in non-permitted regions.

*Models that were considered inadequate.

Source: Survey data, 2022.

domains are characterized by regions I (57-154), II (169-309) and III (372-494) signatures (Lyashenko et al., 2006) is predicted (Zdobnov & Apweiler, 2001) in lacasse sequence of *P. ostreatus*, with 97, 140 and 122 lengths, respectively.

Preparation and prediction of theoretical models of *P. ostreatus* laccase

In the *P. ostreatus* laccase primary structure, a 21aa length in C-terminal was identified out of the main domain. Only conserved domains were considered for molecular modeling. In this sense, the delivered prediction from constraints of spatial restraints (Modeller) approach successively solves the entire target sequence limited by an essentially >30% identity template and >25% R-factor (Ohlendorf, 1994; Šali et al., 1995), while the automated prediction approach (Swiss Model) removed 27 residues length from target sequence in C-terminal region by similarity criteria (Reddy et al., 2015). To all accounts, Wallner and Elofsson (2005) identified a loss of model coordinates in the N-terminal and C-terminal regions in the Swiss-Model, 3D-JIGSAW and Builder programs due to the occurrence of gaps in these regions.

Comparison of refined and unrefined *P. ostreatus* laccase theoretical models

The global quality and stereochemical evaluation of the predicted models, before and after the refinement, are presented in Table 2. Models predicted with the Swiss model approach showed less than 90% of residues in the most

favorable regions, and the proportion of amino acids in these regions increased after refinement but remained below the models predicted by Modeller. In addition, all models predicted in the Swiss model displayed residue in the disallowed regions (RNP), even after refinement. On the other hand, models with favorable stereochemistry were predicted by Modeller with more than 90% of amino acids arranged in the RMF (most favorable region) (Figure S1) only the Lacc1MN, Lacc3MN and Lacc4MN models. After refinement, all models, except for Lacc1SR, showed more than 90% of the amino acids in the RMF (Sarkar et al., 2020; Mehra et al., 2018).

All models showed high similarity between the 3D structure and the amino acid sequence (2D structure), obtaining values greater than 94.3% in verify 3D (Figure S3). The relative frequency of non-covalent interactions between the various types of atoms showed values higher than 81.91 in ERRAT (Figure S4). The comparison between the atomic volumes and the sets of default values pre-calculated in PROVE showed that of the 10 refined models, 4 presented values greater than 5%, which can be considered inadequate (Table 2) (Bowie et al., 1991; Colovos & Yeates, 1993; Laskowski et al., 1993; Pontius et al., 1996; Messaoudi et al., 2013).

Among the unrefined theoretical models, the Lacc4MN stood out, hence it showcased more than 90% of the amino acids in the RMF, as well as 0% of the amino acids in the RNP. These values were associated with high scores in Verify 3D and PROVE, with 98.39 and 3.7%, respectively (Table 2). Among the refined models, Lacc3MR had the highest number of amino acids in the RMF, associated with the lowest number of residues (0.2%) in the RNP and the best scores in Verify 3D and Prove (Table 2).

The models predicted by Modeller showed better structural and stereochemical quality. Thus, the Lacc4MN and Lacc3MR models were selected, and their structure was evaluated. Meshram et al. (2010) predicted a theoretical model of *Pycnoporus cinnabarinus* laccase using the homology modeling technique and compared the same tools that were herein used (i.e., Modeller and Swiss-Model). Their results showed that the models predicted by Modeller are better in terms of performance, geometric and stereochemical properties, thus corroborating to the data obtained in our research.

Structural analysis of Lac4MN and Lac3MR models

The Lacc4MN and Lacc3MR models presented QMEAN Z-scores of -0.98 and 0.17, respectively, hence indicating that they are similar to the structures that were used as template, as well as of adequate structural quality (Benkert et al., 2009).

Visual analysis of the Lacc4MN model (Figure 2) evidenced the interactions between the laccase active site amino acids and copper atoms. According to Zheng et al. (2008), the average distance between the copper ion Cu^{2+} and the nitrogen in the protein models with high resolution present in the PDB is 2.04 Å. The interaction between copper atoms and protein residues occurs through the imidazole moiety of the histidine residue, which yields an adequate environment

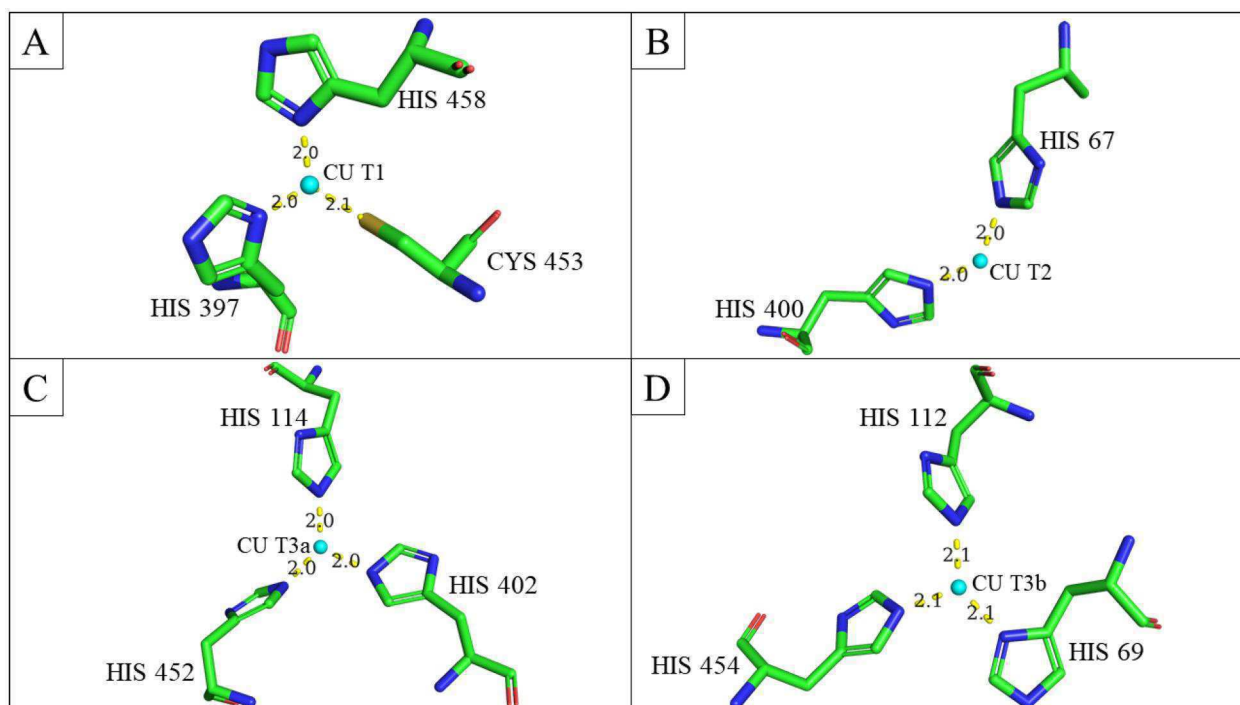


Figure 2. Interactions between amino acids and copper ions from the Lacc4MN model. (A) Cu T1; (B) Cu T2; (C) Cu T3a; (D) Cu T3b. Light blue spheres: copper atoms; In yellow: distances between copper atoms and amino acids. In amino acids—In blue: nitrogen; In green: carbon; In red: oxygen; In yellow: sulfide. Source: Survey data, 2022.

for the establishment of a coordination complex between the nitrogen atoms and the copper. The optimal distance between the nitrogen and copper in these structures according to the Cambridge Structural Database (CSD) ranges from 1.90 to 2.28 Å (Harding, 1999). The distance between Cu T1 and the sulfur present in cysteine is 2.11 Å. After reduction, the Cu–S distance increases to 2.21 Å (Lontie, 1984). In the Lacc4MN model all distances are within the allowed range, showing that all four copper atoms are properly stabilized through interaction with histidine and cysteine. On the other hand, in the Lacc3MR model, the atoms of Cu T1, Cu T2 and Cu T3b were at distances greater than 2.28 Å (Figure 3A, B, and D), and only the interactions of Cu T3a were within this predicted range (Figure 3C).

Upon refinement, it could be seen changes in the distances between copper atoms and amino acids, and the interactions between the copper atoms and the active site amino acids were lost. This is likely because GalaxyRefine server rebuilds and repacks the overall side chains, starting from the center of the protein, and extends to the surface, layer by layer. This causes changes in amino acid positions, even active site amino acids, as described by Heo et al. (2013). In fact, Adiyaman and McGuffin (2019) reported that the refinement can lead to a reduction in the quality of models, and it is necessary to analyze whether the model has been qualitatively improved. Faced with the difficulty of stabilizing the copper atoms in the Lacc3MR model, the other tests were performed with the Lacc4MN model.

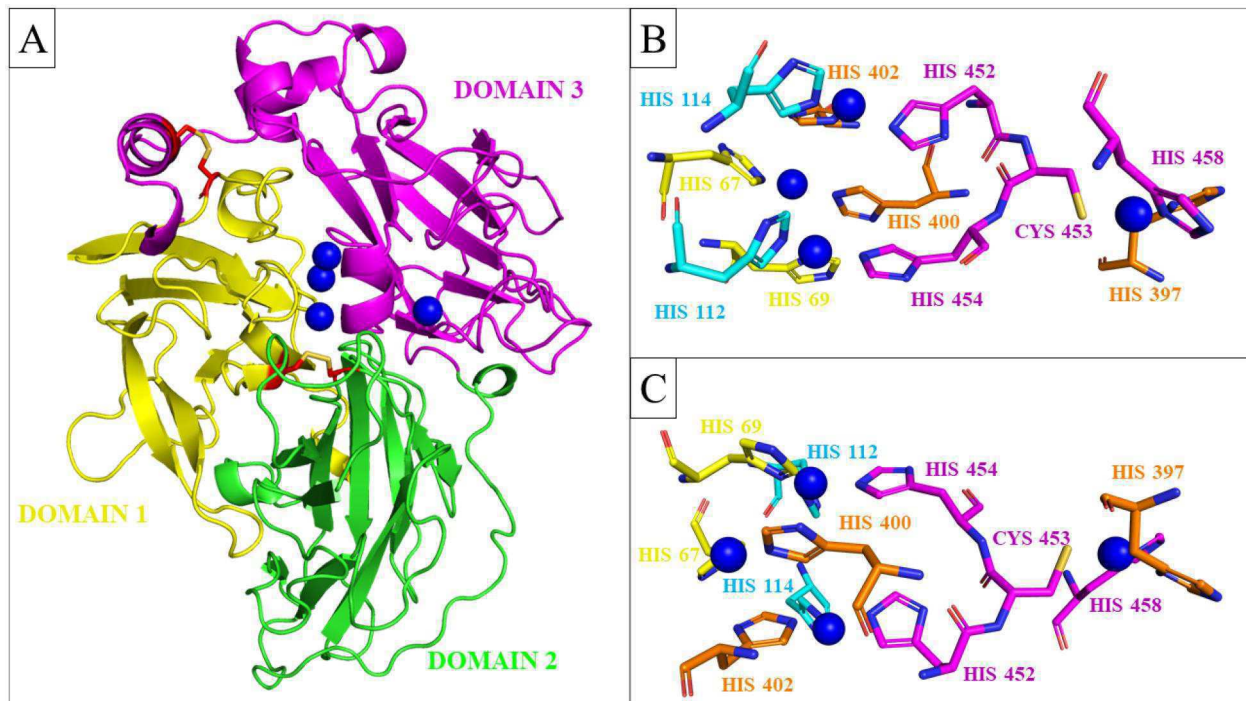
The overlap of the Lacc4MN model and the 4JHU structure confirms the similarity between them (Figure 4A) with RMSD of 0.102 and QMEANDisCo of 0.81 (Studer et al., 2020).

Furthermore, both 3D structures showed similarities in the coordinates of the copper atoms, and in the distance between the nitrogen of the amino acid residue and the copper (Figure 4B, C), with the Cu T1 located close to the surface of the protein.

The three-dimensional structure of *P. ostreatus* Lacc4MN laccase model has 7 β sheets, 8 β staples, 8 β protrusions, 31 β strands, 12 helices, 3 helix-helix interactions, 66 β loops, 7 γ loops, 2 disulfide bridges, in addition to the 4 copper atoms. The high number of β strands causes the formation of Greek key motifs in each of the domains of the Lacc4MN model, which are stabilized by hydrogen bonds between the β sheets. Furthermore, one of the two disulfide bonds present in the Lacc4MN model is located between domains 1 and 3, while the second is between domains 1 and 2 (Figure 5A).

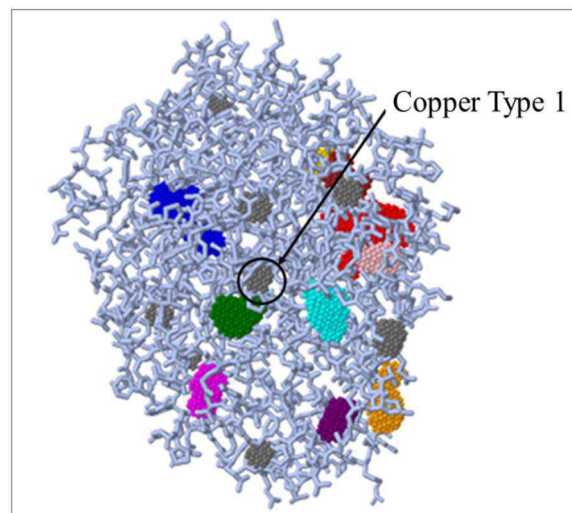
Figure 5B, C show the interactions between the residues of each of the four conserved regions among all the models studied here, according to the multiple alignments (Figure 1) and the copper atoms. The amino acids in the L1 and L2 region interact with the T3 Cu atoms (T3a and T3b), while the L3 and L4 amino acids interact with the T1 and T2 copper atoms, and the T1, T3a and T3b copper atoms, respectively, suggesting the evolutionary importance of these four conserved regions since they directly influence the stabilization of metals in laccase.

The characteristic domains of laccase present an architecture like a Greek key motif (β -barrel) with two β -sheets. Each of these domains is composed of four strands, which likely renders their structure stable. In laccases, the structure is stabilized through the formation of disulfide bridges between



Source: Survey data, 2022.

Figure 5. Domains and disulfide bridges of the three-dimensional model of *P. ostreatus* Lacc4MN laccase. **A:** In yellow: Domain 1; In green: Domain 2; In purple: Domain 3; Cyan spheres: copper atoms; In red: cysteine residues that form the two disulfide bonds. **B:** Zoom in on the copper atoms region showing the interaction with the residues of the conserved regions of the laccase. In blue: copper atoms; In yellow: L1 region; In cyan: L2 region; In orange: L3 region; In purple: L4 region. **C:** View from another angle of copper atoms. Source: Survey data, 2022.



Source: Survey data, 2022.

Figure 6. Possible binding sites according to Ghecom, which were calculated within a 4 Å radius of the Lacc4MN model. In red: site 1; In blue: site 2; In green: site 3; In yellow: site 4; In cyan: site 5. Source: Survey data, 2022.

Table 3. Amino acids that make up the catalytic sites 3 and 5 of the Lacc4MN model were obtained through Ghecom.

Site 3	Site 5
NPV 165; PRO 166; CYS 207; ASP 208; PRO 209; ASN 210; TYR 211; THR 212; GLN 239; PHE 241; ALA 242; GLY 243; ASN 264; PRO 265; ASN 266; LEU 267; GLY 268; VAL 393; GLY 394; GLY 395; PRO 396; HIS 397; PRO 398; ILE 399; NPV 428; SER 429; THR 430; HIS 452; CYS 453; HIS 454; ILE 455; ASP 456; TRP 457; HIS 458; LEU 459.	NPV 225; NPV 235; ASP 236; SER 237; ILE 238; GLN 239; ILE 240; PHE 241; ALA 242; GLY 243; GLN 244; ARG 245; TYR 246; SER 247; ASN 300; PRO 301; LEU 302; ILE 303; GLU 304; THR 305; ASN 306; LEU 307; NPV 308; ARG 410; SER 411; ALA 412; GLY 413; SER 414; SER 415; ARG 424; ARG 425; ASP 426; NPV 427; NPV 428; SER 429; TYR 430; GLY 431; TYR 432; ASN 436; NPV 437; THR 438.

Source: Survey data, 2022.

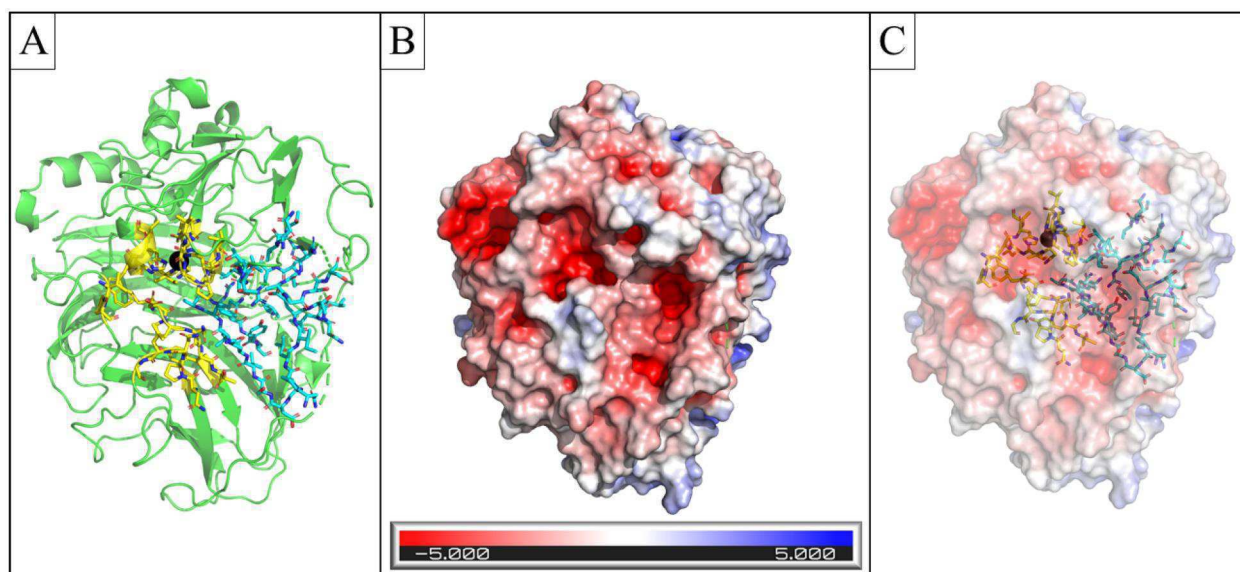


Figure 7. Electrostatic characterization of the Lacc4MN model, visualized in the PyMOL software. (A) residues that make up sites 3 and 5. (B) Electrostatic surface of the Lacc4MN model. (C) Superposition of the electrostatic surface on sites 3 and 5. In green: secondary structures; In yellow: site 3; In cyan: site 5; Electrostatic surface varies between positive charges (blue), neutral charges (white) and negative charges (red). Source: Survey data, 2022.

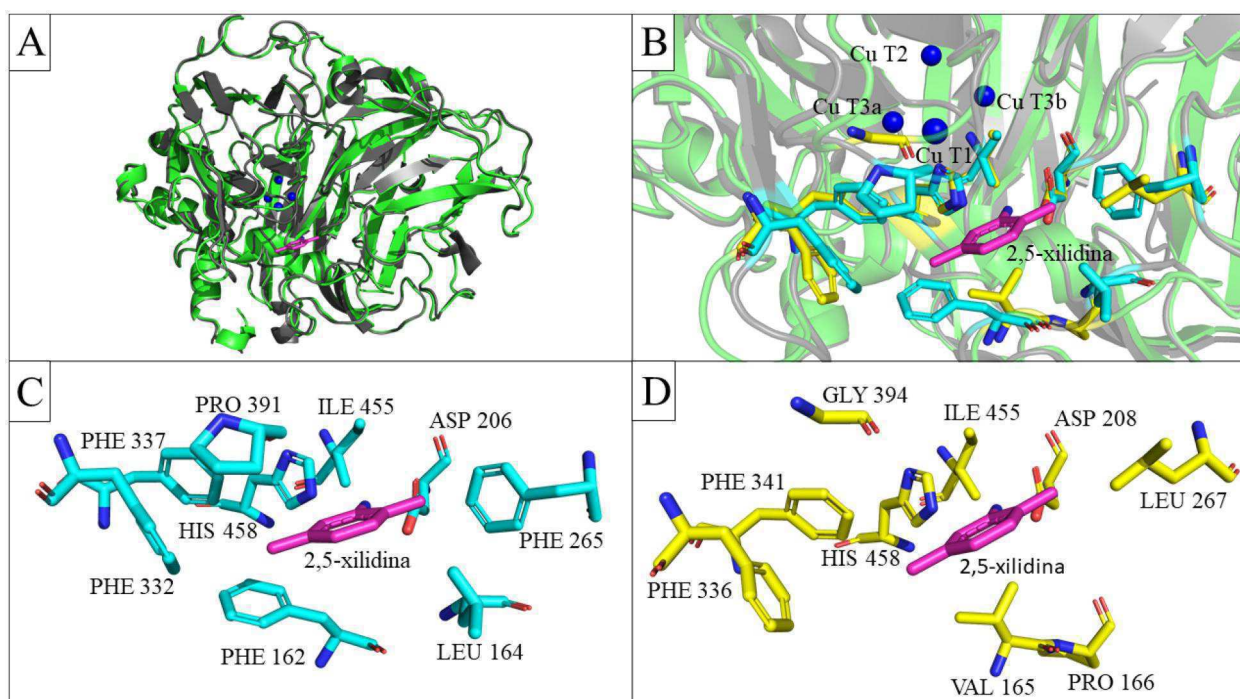


Figure 8. Comparison between the Lacc4MN model and the 1KYA structure, visualized in the PyMOL software. (A) Superposition of the 1KYA crystallographic structures (dark gray) and the theoretical model Lacc4MN (green). Blue spheres: copper atoms; In the pink: 2,5-xylidina. (B) Zoom in on the active site region with the overlap of the residues of the two structures next to 2,5-xylidina. In cyan, the amino acids of the 1KYA structure are represented, and in yellow the amino acids of the Lacc4MN model. (C) Amino acids of the 1KYA structure close to 2,5-xylidina. (D) Amino acids of the Lacc4MN structure close to 2,5-xylidina. Source: Survey data, 2022.

453 and HIS 458 interacting with Cu T1, while HIS 452 and HIS 454 interacting with the T3a and T3b coppers, respectively (Figure 8).

Site 3 is composed of 35 amino acid residues, of which 21 are nonpolar and play an important role in the catalytic site of laccases, hence when a hydrophobic region is close to the copper ion, it causes a relative destabilization of the oxidized copper Cu^{2+} over the reduced copper Cu^{1+} , what results in higher redox potential of the corresponding copper (Gunne

et al., 2014). This demonstrates that the hydrophobic amino acids that are present at the binding site may also be related to the stabilization of the ligand, the protein and the interaction with the anchor residues. However, hydrophilic residues such as aspartic acid and glutamic acid are also important for the catalytic functionality of the active site, as they are generally present in the pocket and act as a proton acceptor during ligand oxidation. The substrate probably loses its proton, and then the electron is captured by the Cu

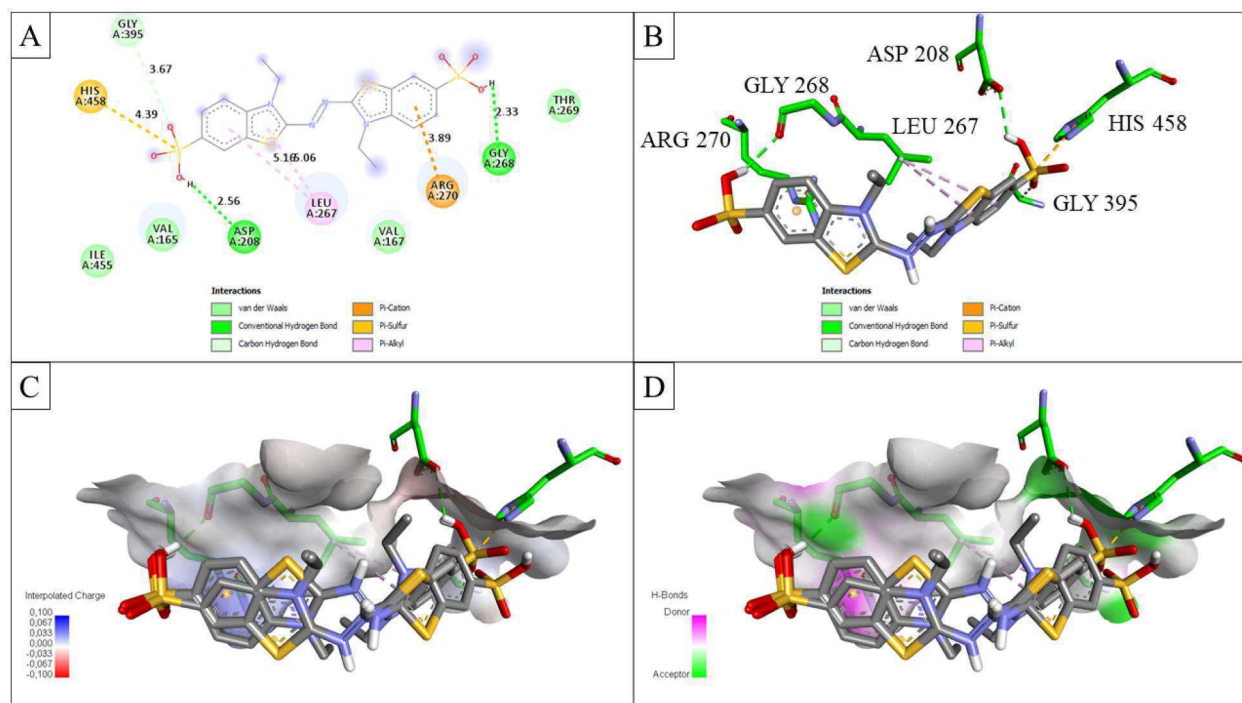


Figure 9. Interactions between the Lacc4MN model and ABTS. (A) Two-dimensional diagram of interactions between the Lacc4MN model and ABTS. (B) Interactions between the Lacc4MN model and ABTS. (C) Bond pocket charges (blue represents positive charge and red represents negative charge). (D) Donors and acceptors of the hydrogen bonds around the bond pocket (green represents the acceptor and purple represents the donor). Source: Survey data, 2022.

T1 via a histidine exposed to the laccase surface (Kallio et al., 2009; Kolyadenko et al., 2021).

A remarkable finding that corroborates the adequacy of the model herein developed is that the active sites are located in electronegative regions (Figure 7). In a study performed with *Trametes versicolor* laccase, it was noted that in a laccase-substrate complex, the substrate binds to a small negatively charged pocket close to Cu T1. The negative charges at this site may have functional significance, as they can stabilize the cationic radical products that are formed during the catalytic cycle (Piontek et al., 2002).

According to Sitarz et al. (2016), the CU T1 site is located in a pocket on the surface of the enzyme, at the interface of domain 3, while the trinuclear copper sites (T2/T3) are positioned between the domains 1 and 3, which provide the ligand residues for the coordination of copper atoms. In fact, the very same observation could be seen in our model (Figure 5A).

The characteristics of site 3 demonstrate that this is probably the catalytic site of the Lacc4MN model. The structure of *Trametes versicolor* laccase 1KYA, which was determined by the X-ray diffraction method under a resolution of 2.40 Å and carried out with a crystallized enzyme linked to 2,5-xylydine, was used to confirm the amino acids that make up the active site of the Lacc4MN model (Figure 8). In this regard, the pocket surrounding the 2,5-xylydine is quite wide, allowing the accommodation of substrates of various sizes. Several amino acid residues make hydrophobic interactions with the aromatic ring of the ligand. Moreover, two polar residues interact with the amino group, the first is a histidine that also coordinates copper (*i.e.*, primary electron acceptor), and the second is an aspartate that is conserved among fungal laccases (Bertrand et al., 2002).

The superposition of the structures showed that both have great structural similarity, with several highly conserved regions (Figure 8A), including in the active site region, since the amino acids close to 2,5-xylydine in the 1KYA model are similar to the amino acids of the site 3 (Figure 8).

Comparing the structure of the laccase obtained experimentally with the theoretical model Lacc4MN, it is possible to suggest that site 3 is possibly the active site of the Lacc4MN model. Among the residues of the 1KYA structure that interact with 2,5-xylydine are HIS 458 and ASP 206, which are involved in electron and proton transfer. Furthermore, xylydine also interacts with the residues: PHE 162, LEU 164, PHE 265, PHE 332, PHE 337, PRO 391 and ILE 455 (Bertrand et al., 2002).

The residues HIS 458 and ASP 208 that make up the active site of the Lacc4MN model are conserved amino acids in all laccases, as seen in the multiple alignment (Figure 1), and the amino acids next to them also show similarity in all sequences, thereby hinting that the structure of the active site is also conserved. The other active site amino acids undergo some mutations, and amino acids PHE 162, LEU 164, PHE 265 and PRO 391 of the 1KYA structure were replaced by VAL 165, PRO 166, LEU 267 and GLY 394 in the Lacc4MN model (Figure 8C, D).

Mohamad et al. (2008) analyzed the active site residues of the 1KYA structure and realized that some residues that are present in the binding site are nonpolar amino acids, such as amino acids PHE 162, LEU 164, PHE 265, PHE 332, PHE 337 and PRO 391. In most cases, these amino acids are replaced by other nonpolar amino acids, as was also identified in this research, being VAL, LEU and GLY, all nonpolar. It is noted that the substitution of amino acids increased the distance

between the residues and the ligand, especially the change of residue PRO 391 for GLY 394, and consequently, there is an increase in the size of the ligation pocket, thereby allowing ligands of higher molecular weight to easily dock at the site region and interact with amino acids. The Lacc4MN model .pdb file can be found in S2.

Molecular docking simulation between laccase and ABTS

The molecular docking simulation between the Lacc4MN model and the ABTS molecule showed binding free energy in the range -4.7 to -3.9 kcal mol⁻¹, as well as the formation of two hydrogen bonds involving the amino acids ASP 208 and GLY 268 (Figure 9), thereby indicating the thermodynamic feasibility of the reaction (Hsu et al., 2012; Sridhar et al., 2013; Ballaminut et al., 2019; Srinivasan et al., 2019). It was observed the formation of five Van der Waals interactions (VAL 165, VAL 167, THR 269, GLY 395 and ILE 455), one carbon-hydrogen bond (GLY 395), two Pi-alkyl interactions (LEU 267), and one Pi-cation interaction (ARG 270) (Figure 9A, B). In the interactions involving ASP 208 and HIS 458 and ABTS, it was noted that these two amino acids act as proton and electron acceptors, respectively (Figure 9C, D).

Between residue HIS 458 and ABTS, a Pi-sulfur bond was established. The Pi-sulfur interaction was tested in biological systems elsewhere and is estimated to contribute with 0.5–2 kcal mol⁻¹ to the binding/stability of the enzyme-substrate complex. Studies involving hydrogen bonds also indicate a contribution between 0.5 and 2 kcal mol⁻¹ for the stability of the interaction (Daeffler et al., 2012), which shows that the Pi-sulfur interaction could be of great importance for the stability of the enzyme-substrate complex. The Lacc4MN model .pdb file can be found in S3.

The docking results mainly demonstrate that the protein predicted model herein maintains the structure and, at a theoretic level, the catalytic functionality that is typical of laccases. Considering that ABTS is one of the main substrates for determining the activity of this enzyme, the docking results offer further data to corroborate with the validation of the model (Christensen & Kepp, 2014; Herrera-Zúñiga et al., 2020).

Conclusion

Modeling a metalloprotein, such as laccase, is a challenging process. The use of different ways to predict the 3D structure of the case of *P. ostreatus* showed that the fully automatic server of the Swiss Model is very attractive for modeling by homology but generates models with low stereochemical quality that require refinement. Concurrently, the refinement of the theoretical 3D models of laccase caused the destabilization of copper atoms. The Modeller program, in turn, required programming knowledge, as well as removing the signal peptide manually and manual adjustments to correct the position of copper atoms. The Modeller program promoted the prediction of theoretical 3D laccase models with better stereochemical characteristics compared to the Swiss Model server without needing refinement. The theoretical 3D model of *P. ostreatus*

laccase (Lacc4MN) presented stereochemical and structural characteristics that allow its use *in silico* tests.

Computational methods make it possible to deepen knowledge about the catalytic mechanisms of enzymes, as in the case of laccase, allowing, through *in silico* studies, the creation of new technologies and value-added products *in vitro* and/or *in vivo* with applications in several areas of industrial interest.

Disclosure statement

The authors report there are no competing interests to declare.

Funding

The authors thank the National Council for Scientific and Technological Development (CNPq) and the Sao Paulo Research Foundation (grant #2021/15022-6) for their support in the development of this research.

ORCID

Marco Antonio Silva  <http://orcid.org/0000-0001-6090-4237>
 José Cordeiro do Nascimento Júnior  <http://orcid.org/0000-0001-5748-9327>
 Douglas Vieira Thomaz  <http://orcid.org/0000-0003-0000-3466>
 Rafael Trindade Maia  <http://orcid.org/0000-0002-5870-1091>
 Vinicius Costa Amador  <http://orcid.org/0000-0002-7946-5665>
 Giovana Tommaso  <http://orcid.org/0000-0002-0933-8855>
 Glauciane Danusa Coelho  <http://orcid.org/0000-0001-9695-0534>

References

- Adiyaman, R., & McGuffin, L. J. (2019). Methods for the refinement of protein structure 3D models. *International Journal of Molecular Sciences*, 20(9), 2301. <https://www.mdpi.com/1422-0067/20/9/2301>. <https://doi.org/10.3390/ijms20092301>
- Altschul, S. F., Madden, T. L., Schäffer, A. A., Zhang, J., Zhang, Z., Miller, W., & Lipman, D. J. (1997). Gapped BLAST and PSI-BLAST: A new generation of protein database search programs. *Nucleic Acids Research*, 25(17), 3389–3402. <https://academic.oup.com/nar/article-lookup/https://doi.org/10.1093/nar/25.17.3389>.
- Álvarez-Machancoses, Ó., Fernández-Martínez, J. L., & Kloczkowski, A. (2020). Prediction of protein tertiary structure via regularized template classification techniques. *Molecules*, 25(11), 2467. <https://www.mdpi.com/1420-3049/25/11/2467>. <https://doi.org/10.3390/molecules25112467>
- Ardila-Leal, L. D., Poutou-Piñales, R. A., Pedroza-Rodríguez, A. M., & Quevedo-Hidalgo, B. E. (2021). A brief history of colour, the environmental impact of synthetic dyes and removal by using laccases. *Molecules*, 26(13), 3813. <https://www.mdpi.com/1420-3049/26/13/3813>. <https://doi.org/10.3390/molecules26133813>
- Arregui, L., Ayala, M., Gómez-Gil, X., Gutiérrez-Soto, G., Hernández-Luna, C. E., Herrera de Los Santos, M., Levin, L., Rojo-Domínguez, A., Romero-Martínez, D., Saparrat, M. C. N., Trujillo-Roldán, M. A., & Valdez-Cruz, N. A. (2019). laccases: Structure, function, and potential application in water bioremediation. *Microbial Cell Factories*, 18(1), 200. <https://microbialcellfactories.biomedcentral.com/articles/https://doi.org/10.1186/s12934-019-1248-0>.
- Awasthi, M., Jaiswal, N., Singh, S., Pandey, V. P., & Dwivedi, U. N. (2015). Molecular docking and dynamics simulation analyzes unraveling the differential enzymatic catalysis by plant and fungal laccases with respect to lignin biosynthesis and degradation. *Journal of Biomolecular Structure & Dynamics*, 33(9), 1835–1849. <https://doi.org/10.1080/07391102.2014.975282>
- Ballaminut, N., Coelho, G. D., Maia, R. T., Vitali, V. M. V., Matheus, D. R. (2019). In vitro and in silico decolorization of reactive dye by

- basidiomycete fungus laccase. In *Knowledge, Conservation and Use of Fungi* (vol. 1, pp. 107–115).
- Benkert, P., Künzli, M., & Schwede, T. (2009). QMEAN server for protein model quality estimation. *Nucleic Acids Research*, 37(Web Server issue), W510–14. <https://academic.oup.com/nar/article-lookup/>. <https://doi.org/10.1093/nar/gkp322>
- Bertrand, T., Jolival, C., Briozzo, P., Caminade, E., Joly, N., Madzak, C., & Mougou, C. (2002). Crystal structure of a four-copper laccase complexed with an arylamine: Insights into substrate recognition and correlation with kinetics. *Biochemistry*, 41(23), 7325–7333. <https://pubs.acs.org/>. <https://doi.org/10.1021/bi0201318>
- Bezerra, T. M. d S., Bassan, J. C., Santos, V. T. d O., Ferraz, A., & Monti, R. (2015). Covalent immobilization of laccase in green coconut fiber and use in clarification of apple juice. *Process Biochemistry*, 50(3), 417–423. <https://linkinghub.elsevier.com/retrieve/pii/S1359511314006023>. <https://doi.org/10.1016/j.procbio.2014.12.009>
- Bienert, S., Waterhouse, A., de Beer, T. A. P., Tauriello, G., Studer, G., Bordoli, L., & Schwede, T. (2017). The SWISS-MODEL Repository—New features and functionality. *Nucleic Acids Research*, 45(D1), D313–D319. <https://academic.oup.com/nar/article-lookup/>. <https://doi.org/10.1093/nar/gkw1132>
- Bongirwar, V., & Mokhadde, A. S. (2022). Different methods, techniques and their limitations in protein structure prediction: A review. *Progress in Biophysics and Molecular Biology*, 173, 72–82. <https://doi.org/10.1016/j.pbiomolbio.2022.05.002>
- Bowie, J. U., Luthy, R., & Eisenberg, D. (1991). A method to identify protein sequences that fold into a known three-dimensional structure. *Science (New York, N.Y.)*, 253(5016), 164–170. <https://www.science-mag.org/lookup/>. <https://doi.org/10.1126/science.1853201>
- Brugnerotto, P., Silva, T. R., Brondani, D., Zapp, E., & Vieira, I. C. (2017). Gold nanoparticles stabilized in β -cyclodextrin and decorated with laccase applied in the construction of a biosensor for rutin. *Electroanalysis*, 29(4), 1031–1037. <https://onlinelibrary.wiley.com/>. <https://doi.org/10.1002/elan.201600697>
- Chou, K.-C. (2004). Structural bioinformatics and its impact to biomedical science. *Current Medicinal Chemistry*, 11(16), 2105–2134. <http://www.eurekaselect.com/openurl/content.php?genre=article&issn=0929-8673&volume=11&issue=16&spage=2105>. <https://doi.org/10.2174/0929867043364667>
- Christensen, N. J., & Kepp, K. P. (2014). Setting the stage for electron transfer: Molecular basis of ABTS-binding to four laccases from *trametes versicolor* at variable pH and protein oxidation state. *Journal of Molecular Catalysis B: Enzymatic*, 100, 68–77. <https://linkinghub.elsevier.com/retrieve/pii/S1381117713003469>. <https://doi.org/10.1016/j.molcatb.2013.11.017>
- Chung, S. Y., & Subbiah, S. (1996). A Structural explanation for the twilight zone of protein sequence homology. *Structure (London, England: 1993)*, 4(10), 1123–1127. [https://doi.org/10.1016/S0969-2126\(96\)00119-0](https://doi.org/10.1016/S0969-2126(96)00119-0)
- Coelho, G. D., Silva, K. K., Silva, D. P., Soares, J. K., Ballaminut, N., & Thomaz, D. V. (2020). Biodegradation of synthetic effluent containing CI direct red 28 (Congo Red) by *Lentinus Sp.* laccase leads to low ecotoxicity. *Current Biotechnology*, 9(2), 127–133. <https://doi.org/10.2174/2211550109999200720162021>
- Colovos, C., & Yeates, T. O. (1993). Verification of protein structures: Patterns of nonbonded atomic interactions. *Protein Science*, 2(9), 1511–1519. <http://doi.wiley.com/>. <https://doi.org/10.1002/pro.5560020916>
- Daeflfer, K. N.-M., Lester, H. A., & Dougherty, D. A. (2012). Functionally important aromatic-aromatic and sulfur- π interactions in the D2 dopamine receptor. *Journal of the American Chemical Society*, 134(36), 14890–14896. <https://pubs.acs.org/>. <https://doi.org/10.1021/ja304560x>
- Daronch, N. A., Kelbert, M., Pereira, C. S., de Araújo, P. H. H., & de Oliveira, D. (2020). Elucidating the choice for a precise matrix for laccase Immobilization: A review. *Chemical Engineering Journal*, 397, 125506. <https://linkinghub.elsevier.com/retrieve/pii/S138589472031634X>. <https://doi.org/10.1016/j.cej.2020.125506>
- De la Mora, E., Lovett, J. E., Blanford, C. F., Garman, E. F., Valderrama, B., & Rudino-Pinera, E. (2012). Structural changes caused by radiation-induced reduction and radiolysis: The effect of X-ray absorbed dose in a fungal multicopper oxidase. *Acta Crystallographica. Section D, Biological Crystallography*, 68(Pt 5), 564–577. <http://scripts.iucr.org/cgi-bin/paper?S0907444912005343>. <https://doi.org/10.1107/S0907444912005343>
- de Salas, F., Pardo, I., Salavagione, H. J., Aza, P., Amougí, E., Vind, J., Martínez, A. T., & Camarero, S. (2016). “Advanced Synthesis of Conductive Polyaniline Using laccase as Biocatalyst” ed. Rafael Vazquez-Duhalt. *PLoS One*, 11(10), e0164958. <https://dx.plos.org/>. <https://doi.org/10.1371/journal.pone.0164958>
- Fiser, A., Do, R. K., & Sali, A. (2000). Modeling of loops in protein structures. *Protein Science*, 9(9), 1753–1773. <https://doi.org/10.1110/ps.9.9.1753>
- Fiser, A. (2017). Comparative protein structure modeling. In *From protein structure to function with bioinformatics* (pp. 91–134) Springer Netherlands. <http://link.springer.com/>.
- Fu, N., Li, J., Wang, M., Ren, L., & Luo, Y. (2020). Genes identification, molecular docking and dynamics simulation analysis of laccases from *amylostereum areolatum* provides molecular basis of laccase bound to lignin. *International Journal of Molecular Sciences*, 21(22), 8845. <https://www.mdpi.com/1422-0067/21/22/8845>. <https://doi.org/10.3390/ijms21228845>
- Giacobelli, V. G., Monza, E., Fatima Lucas, M., Pezzella, C., Piscitelli, A., Guallar, V., & Sannia, G. (2017). Repurposing designed mutants: a valuable strategy for computer-aided laccase engineering – the case of POXA1b. *Catalysis Science & Technology*, 7(2), 515–523. <http://xlink.rsc.org/?DOI=C6CY02410F>. <https://doi.org/10.1039/C6CY02410F>
- Glazunova, O. A., Polyakov, K. M., Fedorova, T. V., Dorovatovskii, P. V., & Koroleva, O. V. (2015). Elucidation of the crystal structure of *Coriopsis Caperata* laccase: Restoration of the structure and activity of the native enzyme from the T2-depleted form by copper ions. *Acta Crystallographica. Section D, Biological Crystallography*, 71(Pt 4), 854–861. <http://scripts.iucr.org/cgi-bin/paper?S1399004715001595>. <https://doi.org/10.1107/S1399004715001595>
- Guex, N., & Peitsch, M. C. (1997). SWISS-MODEL and the Swiss-PdbViewer: An environment for comparative protein modeling. *Electrophoresis*, 18(15), 2714–2723. <https://doi.org/10.1002/elps.1150181505>
- Gunne, M., Höppner, A., Hagedoorn, P.-L., & Urlacher, V. B. (2014). Structural and redox properties of the small laccase Ssl1 from *Streptomyces Svicesus*. *The FEBS Journal*, 281(18), 4307–4318. <https://onlinelibrary.wiley.com/>. <https://doi.org/10.1111/febs.12755>
- Harding, M. M. (1999). The geometry of metal-ligand interactions relevant to proteins. *Acta Crystallographica. Section D, Biological Crystallography*, 55(Pt 8), 1432–1443. <http://scripts.iucr.org/cgi-bin/paper?S0907444999007374>. <https://doi.org/10.1107/s0907444999007374>
- Heo, L., Park, H., & Seok, C. (2013). GalaxyRefine: Protein structure refinement driven by side-chain repacking. *Nucleic Acids Research*, 41(Web Server issue), W384–88. <http://academic.oup.com/nar/article/41/W1/W384/1108398/GalaxyRefine-protein-structure-refinement-driven>. <https://doi.org/10.1093/nar/gkt458>
- Herrera-Zúñiga, L. D., González-Palma, M., Díaz-Godínez, G., Martínez-Carrera, D. C., Sánchez-Hernández, M. C., & Díaz-Godínez, R. (2020). Molecular docking of oxidases from *pleurotus ostreatus* and the activity of those produced by ARS 3526 strain grown in both, submerged and solid-state fermentations. *Revista Mexicana de Ingeniería Química*, 20(1), 453–466. <http://rmiq.org/ojs311/index.php/rmiq/article/view/2076>. <https://doi.org/10.24275/rmiq/Bio2076>
- Hsu, C.-A., Wen, T.-N., Su, Y.-C., Jiang, Z.-B., Chen, C.-W., & Shyur, L.-F. (2012). Biological degradation of anthroquinone and azo dyes by a novel laccase from *Lentinus Sp.* *Environmental Science & Technology*, 46(9), 5109–5117. <https://doi.org/10.1021/es2047014>
- Hublik, G., & Schinner, F. (2000). Characterization and immobilization of the laccase from *Pleurotus Ostreatus* and its use for the continuous elimination of phenolic pollutants. *Enzyme and Microbial Technology*, 27(3-5), 330–336. <https://linkinghub.elsevier.com/retrieve/pii/S0141022900002209>. [https://doi.org/10.1016/S0141-0229\(00\)00220-9](https://doi.org/10.1016/S0141-0229(00)00220-9)
- Jang, W. D., Lee, S. M., Kim, H. U., & Lee, S. Y. (2020). Systematic and comparative evaluation of software programs for template-based modeling of protein structures. *Biotechnology Journal*, 15(6), 1900343. <https://onlinelibrary.wiley.com/>. <https://doi.org/10.1002/biot.201900343>

- Kallio, J. P., Auer, S., Jänis, J., Andberg, M., Kruus, K., Rouvinen, J., Koivula, A., & Hakulinen, N. (2009). Structure–function studies of a melanocarpus albomyces laccase suggest a pathway for oxidation of phenolic compounds. *Journal of Molecular Biology*, 392(4), 895–909. <https://linkinghub.elsevier.com/retrieve/pii/S0022283609007736>. <https://doi.org/10.1016/j.jmb.2009.06.053>
- Kaur, T., Madgulkar, A., Bhalekar, M., & Asgaonkar, K. (2019). Molecular docking in formulation and development. *Current Drug Discovery Technologies*, 16(1), 30–39. <http://www.eurekaselect.com/159908/article>. <https://doi.org/10.2174/1570163815666180219112421>
- Kawabata, T., & Go, N. (2007). Detection of pockets on protein surfaces using small and large probe spheres to find putative ligand binding sites. *Proteins*, 68(2), 516–529. <http://doi.wiley.com/>. <https://doi.org/10.1002/prot.21283>
- Khatami, S. H., Vakili, O., Movahedpour, A., Ghesmati, Z., Ghasemi, H., & Taheri-Anganeh, M. (2022). laccase: Various types and applications. *Biotechnology and Applied Biochemistry*, 1–15. <https://onlinelibrary.wiley.com/>. <https://doi.org/10.1002/bab.2313>
- Kim, S., Chen, J., Cheng, T., Gindulyte, A., He, J., He, S., Li, Q., Shoemaker, B. A., Thiessen, P. A., Yu, B., Zaslavsky, L., Zhang, J., & Bolton, E. E. (2021). PubChem in 2021: New data content and improved web interfaces. *Nucleic Acids Research*, 49(D1), D1388–D1395. <https://academic.oup.com/nar/article/49/D1/D1388/5957164>. <https://doi.org/10.1093/nar/gkaa971>
- Kolyadenko, I., Scherbakova, A., Kovalev, K., Gabdulkhakov, A., & Tishchenko, S. (2021). Engineering the catalytic properties of two-domain laccase from *Streptomyces Griseoflavus* Ac-993. *International Journal of Molecular Sciences*, 23(1), 65. <https://www.mdpi.com/1422-0067/23/1/65>. <https://doi.org/10.3390/ijms23010065>
- Koonin, E. V., & Galperin, M. Y. (2003). Evolutionary concept in genetics and genomics. In *Sequence - Evolution - Function: Computational Approaches in Comparative Genomics* (pp. 25–49) Springer Science + Business Media, LLC. <https://www.ncbi.nlm.nih.gov/books/NBK20255/>.
- Kumar, A. K., & Sharma, S. (2017). Recent updates on different methods of pretreatment of lignocellulosic feedstocks: A review. *Bioresources and Bioprocessing*, 4(1), 7. <http://bioresources.bioprocessing.springeropen.com/articles/>. <https://doi.org/10.1186/s40643-017-0137-9>
- Kumar, S. S., Phale, P. S., Durani, S., & Wangikar, P. P. (2003). Combined sequence and structure analysis of the fungal laccase family. *Biotechnology and Bioengineering*, 83(4), 386–394. <http://doi.wiley.com/>. <https://doi.org/10.1002/bit.10681>
- Laskowski, R. A., Jablonska, J., Pravda, L., Vařeková, R. S., & Thornton, J. M. (2018). PDBsum: Structural summaries of PDB entries. *Protein Science*, 27(1), 129–134. <https://onlinelibrary.wiley.com/10.1002/pro.3289>.
- Laskowski, R. A., MacArthur, M. W., Moss, D. S., & Thornton, J. (1993). PROCHECK: A program to check the stereochemical quality of protein structures. *Journal of Applied Crystallography*, 26(2), 283–291. <http://scripts.iucr.org/cgi-bin/paper/S0021889892009944>. <https://doi.org/10.1107/S0021889892009944>
- Leonowicz, A., Cho, N., Luterek, J., Wilkolazka, A., Wojtas-Wasilewska, M., Matuszewska, A., Hofrichter, M., Wesenberg, D., & Rogalski, J. (2001). Fungal laccase: Properties and activity on lignin. *Journal of Basic Microbiology*, 41(3–4), 185–227. <https://onlinelibrary.wiley.com/>. [https://doi.org/10.1002/1521-4028\(200107\)41:3/4%3C185::AID-JOBM185%3E3.O.CO;2-T](https://doi.org/10.1002/1521-4028(200107)41:3/4%3C185::AID-JOBM185%3E3.O.CO;2-T)
- Leynaud Kieffer Curran, L. M. C., Pham, L. T. M., Sale, K. L., & Simmons, B. A. (2022). Review of advances in the development of laccases for the valorization of lignin to enable the production of lignocellulosic biofuels and bioproducts. *Biotechnology Advances*, 54, 107809. <https://linkinghub.elsevier.com/retrieve/pii/S0734975021001154>. <https://doi.org/10.1016/j.biotechadv.2021.107809>
- Lontie, R. (1984). *Copper proteins and copper enzymes* (1st ed.). CRC Press. <https://www.taylorfrancis.com/books/9781351079358>
- Lyashenko, A. V., Zhukhlistova, N. E., Gabdulkhakov, A. G., Zhukova, Y. N., Voelter, W., Zaitsev, V. N., Bento, I., Stepanova, E. V., Kachalova, G. S., Koroleva, O. V., Cherkashyn, E. A., Tishkov, V. I., Lamzin, V. S., Schirwitz, K., Morgunova, E. Y., Betzel, C., Lindley, P. F., & Mikhailov, A. M. (2006). Purification, crystallization and preliminary X-ray study of the fungal laccase from *Cerrena Maxima*. *Acta Crystallographica. Section F, Structural Biology and Crystallization Communications*, 62(Pt 10), 954–957. <https://doi.org/10.1107/S1744309106036578>
- Lyashenko, A. V., Bento, I., Zaitsev, V. N., Zhukhlistova, N. E., Zhukova, Y. N., Gabdulkhakov, A. G., Morgunova, E. Y., Voelter, W., Kachalova, G. S., Stepanova, E. V., Koroleva, O. V., Lamzin, V. S., Tishkov, V. I., Betzel, C., Lindley, P. F., & Mikhailov, A. M. (2006). X-ray structural studies of the fungal laccase from *cerrena maxima*. *Journal of Biological Inorganic Chemistry : JBIC*, 11(8), 963–973. <https://doi.org/10.1007/s00775-006-0158-x>
- Maestre-Reyna, M., Liu, W.-C., Jeng, W.-Y., Lee, C.-C., Hsu, C.-A., Wen, T.-N., Wang, A. H.-J., & Shyur, L.-F. (2015). “Structural and Functional Roles of Glycosylation in Fungal laccase from *Lentinus* Sp.” ed. Claudio M Soares. *PLoS One*, 10(4), e0120601. <https://dx.plos.org/>. <https://doi.org/10.1371/journal.pone.0120601>
- Maia, R. T., de Araújo Campos, M., & de Moraes Filho, R. M. (2021). Introductory chapter: homology modeling. In *Homology molecular modeling - perspectives and applications*. IntechOpen. <https://www.intechopen.com/books/homology-molecular-modeling-perspectives-and-applications/introductory-chapter-homology-modeling>
- Mäkelä, M. R., Tuomela, M., Hatakka, A., & Hildén, K. (2020). Fungal laccases and Their Potential in Bioremediation Applications. In *Laccases in bioremediation and waste valorisation* (pp. 1–5). Springer. <http://link.springer.com/>
- Mansur, M., Arias, M. E., Copa-Patiño, J. L., Flärdh, M., & González, A. E. (2003). The white-rot fungus *pleurotus ostreatus* secretes laccase isozymes with different substrate specificities. *Mycologia*, 95(6), 1013–1020. <https://www.tandfonline.com/>. <https://doi.org/10.1080/15572536.2004.11833017>
- Martínková, L., Krístková, B., & Křen, V. (2022). laccases and tyrosinases in organic synthesis. *International Journal of Molecular Sciences*, 23(7), 3462. <https://www.mdpi.com/1422-0067/23/7/3462>. <https://doi.org/10.3390/ijms23073462>
- Martí-Renom, M. A., Stuart, A. C., Fiser, A., Sánchez, R., Melo, F., & Sali, A. (2000). Comparative protein structure modeling of genes and genomes. *Annual Review of Biophysics and Biomolecular Structure*, 29(1), 291–325. <http://www.annualreviews.org/>. <https://doi.org/10.1146/annurev.biophys.29.1.291>
- Masjoudi, M., Golgoli, M., Ghobadi Nejad, Z., Sadeghzadeh, S., & Borghei, S. M. (2021). Pharmaceuticals removal by immobilized laccase on polyvinylidene fluoride nanocomposite with multi-walled carbon nanotubes. *Chemosphere*, 263, 128043. <https://linkinghub.elsevier.com/retrieve/pii/S0045653520322384>. <https://doi.org/10.1016/j.chemosphere.2020.128043>
- Matera, I., Gullotto, A., Tilli, S., Ferraroni, M., Scozzafava, A., & Briganti, F. (2008). Crystal structure of the blue multicopper oxidase from the white-rot fungus *Trametes trogii* complexed with p-toluate. *Inorganica Chimica Acta*, 361(14–15), 4129–4137. <https://linkinghub.elsevier.com/retrieve/pii/S0020169308002697>. <https://doi.org/10.1016/j.ica.2008.03.091>
- Mehra, R., Muschiol, J., Meyer, A. S., & Kepp, K. P. (2018). A structural-chemical explanation of fungal laccase activity. *Scientific Reports*, 8(1), 17285. <https://doi.org/10.1038/s41598-018-35633-8>
- Meshram, R. J., Gavhane, A., Gaikar, R., Bansode, T., Maskar, A., Gupta, A., Sohni, S., Patidar, M., Pandey, T., & Jangle, S. (2010). Sequence analysis and homology modeling of laccase from *pyncoporus cinnabarinus*. *Bioinformation*, 5(4), 150–154. <http://www.bioinformation.net/005/003300052010.htm>. <https://doi.org/10.6026/97320630005150>
- Messaoudi, A., Belguith, H., & Ben Hamida, J. (2013). Homology modeling and virtual screening approaches to identify potent inhibitors of VEB-1 β -lactamase. *Theoretical Biology & Medical Modelling*, 10(1), 22. <https://tbiomed.biomedcentral.com/articles/https://doi.org/10.1186/1742-4682-10-22>
- Miyazawa, N., Tanaka, M., Hakamada, M., & Mabuchi, M. (2017). Molecular dynamics study of laccase immobilized on self-assembled monolayer-modified Au. *Journal of Materials Science*, 52(21), 12848–12853. <http://link.springer.com/>. <https://doi.org/10.1007/s10853-017-1392-z>
- Mohamad, S. B., Ong, A. L., & Ripen, A. M. (2008). Evolutionary trace analysis at the ligand binding site of laccase. *Bioinformation*, 2(9),

- 369–372. <http://www.bioinformatics.net/002/008100022008.htm>. <https://doi.org/10.6026/97320630002369>
- Mot, A.-C., & Silaghi-Dumitrescu, R. (2012). laccases: Complex architectures for one-electron oxidations. *Biochemistry. Biokhimiia*, 77(12), 1395–1407. <http://link.springer.com/https://doi.org/10.1134/S0006297912120085>.
- Ohlendorf, D. H. (1994). Accuracy of refined protein structures. II. Comparison of four independently refined models of human interleukin 1 β . *Acta Crystallographica. Section D, Biological Crystallography*, 50(Pt 6), 808–812. <https://doi.org/10.1107/S0907444994002659>
- Palmieri, G., Giardina, P., Bianco, C., Scaloni, A., Capasso, A., & Sanna, G. (1997). A novel white laccase from *Pleurotus ostreatus*. *The Journal of Biological Chemistry*, 272(50), 31301–31307. <https://linkinghub.elsevier.com/retrieve/pii/S0021925819887525>. <https://doi.org/10.1074/jbc.272.50.31301>
- Pettersen, E. F., Goddard, T. D., Huang, C. C., Couch, G. S., Greenblatt, D. M., Meng, E. C., & Ferrin, T. E. (2004). UCSF chimera? A visualization system for exploratory research and analysis. *Journal of Computational Chemistry*, 25(13), 1605–1612. <https://onlinelibrary.wiley.com/> <https://doi.org/10.1002/jcc.20084>.
- Piontek, K., Antorini, M., & Choinowski, T. (2002). Crystal structure of a laccase from the Fungus *Trametes Versicolor* at 1.90-Å resolution containing a full complement of coppers. *The Journal of Biological Chemistry*, 277(40), 37663–37669. <https://linkinghub.elsevier.com/retrieve/pii/S0021925818364937>. <https://doi.org/10.1074/jbc.M204571200>
- Pontius, J., Richelle, J., & Wodak, S. J. (1996). Deviations from standard atomic volumes as a quality measure for protein crystal structures. *Journal of Molecular Biology*, 264(1), 121–136. <https://linkinghub.elsevier.com/retrieve/pii/S0022283696906282>. <https://doi.org/10.1006/jmbi.1996.0628>
- Reddy, A. R., Venkateswarulu, T. C., Dulla, J. B., & Mikkili, I. (2015). Homology modeling studies of human genome receptor using modeller, Swiss-model server and esypred-3D tools. *International Journal of Pharmaceutical Sciences Review and Research*, 30(1), 1–6.
- Ren, Y., & Yuan, Q. (2015). Fungi in landfill leachate treatment process. In *Biodegradation and bioremediation of polluted systems - new advances and technologies*. InTech. <http://www.intechopen.com/books/biodegradation-and-bioremediation-of-polluted-systems-new-advances-and-technologies/fungi-in-landfill-leachate-treatment-process>.
- Rostami, A., Abdelrasoul, A., Shokri, Z., & Shirvandi, Z. (2022). Applications and mechanisms of free and immobilized laccase in detoxification of phenolic compounds — A review. *Korean Journal of Chemical Engineering*, 39(4), 821–832. <https://link.springer.com/https://doi.org/10.1007/s11814-021-0984-0>
- Šali, A., Potterton, L., Yuan, F., van Vlijmen, H., & Karplus, M. (1995). Evaluation of comparative protein modeling by MODELLER. *Proteins: Structure, Function, and Genetics*, 23(3), 318–326. <https://doi.org/10.1002/prot.340230306>
- Šali, A., & Blundell, T. L. (1993). Comparative protein modeling by satisfaction of spatial restraints. *Journal of Molecular Biology*, 234(3), 779–815. <https://linkinghub.elsevier.com/retrieve/pii/S0022283683716268>. <https://doi.org/10.1006/jmbi.1993.1626>
- Sarkar, S., Banerjee, A., Chakraborty, N., Soren, K., Chakraborty, P., & Bandopadhyay, R. (2020). Structural-functional analyses of textile dye degrading azoreductase, laccase and peroxidase: a comparative in silico study. *Electronic Journal of Biotechnology*, 43, 48–54. <https://doi.org/10.1016/j.ejbt.2019.12.004>
- Singh, D., & Gupta, N. (2020). Microbial laccase: A robust enzyme and its industrial applications. *Biologia*, 75(8), 1183–1193. <http://link.springer.com/> <https://doi.org/10.2478/s11756-019-00414-9>
- Sitarz, A. K., Mikkelsen, J. D., & Meyer, A. S. (2016). Structure, functionality and tuning up of laccases for lignocellulose and other industrial applications. *Critical Reviews in Biotechnology*, 36(1), 70–86. <http://www.tandfonline.com/> <https://doi.org/10.3109/07388551.2014.949617>.
- Sridhar, S., Chinnathambi, V., Arumugam, P., & Suresh, P. K. (2013). In silico and in vitro physicochemical screening of *Rigidoporus sp.* crude laccase-assisted decolorization of synthetic dyes—approaches for a cost-effective enzyme-based remediation methodology. *Applied Biochemistry and Biotechnology*, 169(3), 911–922. <http://link.springer.com/https://doi.org/10.1007/s12010-012-0041-x>.
- Srinivasan, S., Sadasivam, S. K., Gunalan, S., Shanmugam, G., & Kothandan, G. (2019). Application of docking and active site analysis for enzyme linked biodegradation of textile dyes. *Environmental Pollution (Barking, Essex : 1987)*, 248, 599–608. <https://linkinghub.elsevier.com/retrieve/pii/S0269749118357427>. <https://doi.org/10.1016/j.envpol.2019.02.080>
- Studer, G., Rempfer, C., Waterhouse, A. M., Gumienny, R., Haas, J., & Schwede, T. (2020). QMEANDisCo—Distance Constraints Applied on Model Quality Estimation” ed. Arne Elofsson. *Bioinformatics*, 36(6), 1765–1771. <https://academic.oup.com/bioinformatics/article/36/6/1765/5614424>. <https://doi.org/10.1093/bioinformatics/btz828>
- Thakuria, B., Jungai, N., & Adhikari, S. (2015). Catalytic site prediction of azoreductase enzyme of *E. coli* with potentially important industrial dyes using molecular docking tools. *International Journal of Bioscience, Biochemistry and Bioinformatics*, 5(2), 91–99. <https://doi.org/10.17706/ijbb.2015.5.2.91-99>
- Thangudu, R. R., Manoharan, M., Srinivasan, N., Cadet, F., Sowdhamini, R., & Offmann, B. (2008). Analysis on conservation of disulphide bonds and their structural features in homologous protein domain families. *BMC Structural Biology*, 8(1), 55. <https://bmcstructbiol.biomedcentral.com/articles/https://doi.org/10.1186/1472-6807-8-55>.
- Thompson, J. D., Higgins, D. G., & Gibson, T. J. (1994). CLUSTAL W: Improving the sensitivity of progressive multiple sequence alignment through sequence weighting, position-specific gap penalties and weight matrix choice. *Nucleic Acids Research*, 22(22), 4673–4680. <https://academic.oup.com/nar/article-lookup/> <https://doi.org/10.1093/nar/22.22.4673>.
- Trott, O., & Olson, A. J. (2009). AutoDock Vina: Improving the speed and accuracy of docking with a new scoring function, efficient optimization, and multithreading. *Journal of Computational Chemistry*, 31(2), 455–461. <https://onlinelibrary.wiley.com/> <https://doi.org/10.1002/jcc.21334>
- Villalba-Rodríguez, A. M., Parra-Arroyo, L., González-González, R. B., Parra-Saldívar, R., Bilal, M., & Iqbal, H. M. (2022). Laccase-assisted biosensing constructs – robust modalities to detect and remove environmental contaminants. *Case Studies in Chemical and Environmental Engineering*, 5, 100180. <https://linkinghub.elsevier.com/retrieve/pii/S266601642200020>. <https://doi.org/10.1016/j.csee.2022.100180>
- Wallner, B., & Elofsson, A. (2005). All are not equal: A benchmark of different homology modeling programs. *Protein Science*, 14(5), 1315–1327. <http://doi.wiley.com/https://doi.org/10.1110/ps.041253405>.
- Waterhouse, A., Bertoni, M., Bienert, S., Studer, G., Tauriello, G., Gumienny, R., Heer, F. T., de Beer, T. A. P., Rempfer, C., Bordoli, L., Lepore, R., & Schwede, T. (2018). SWISS-MODEL: Homology modeling of protein structures and complexes. *Nucleic Acids Research*, 46(W1), W296–W303. <https://academic.oup.com/nar/article/46/W1/W296/5000024>. <https://doi.org/10.1093/nar/gky427>
- Webb, B., & Sali, A. (2016). Comparative protein structure modeling using MODELLER. *Current Protocols in Bioinformatics*, 54, 5.6.1–5.6.37. <https://onlinelibrary.wiley.com/> <https://doi.org/10.1002/cpbi.3>
- Wu, M.-H., Lee, C.-C., Hsiao, A.-S., Yu, S.-M., Wang, A. H.-J., & Ho, T.-H. D. (2018). Kinetic Analysis and Structural Studies of a High-efficiency laccase from *Cerrena Sp.* RSD 1. *FEBS Open Bio*, 8(8), 1230–1246. <https://onlinelibrary.wiley.com/> <https://doi.org/10.1002/2211-5463.12459>.
- Zdobnov, E. M., & Apweiler, R. (2001). InterProScan - an integration platform for the signature-recognition methods in InterPro. *Bioinformatics (Oxford, England)*, 17(9), 847–848. <https://academic.oup.com/bioinformatics/article-lookup/> <https://doi.org/10.1093/bioinformatics/17.9.847>.
- Zerva, A., Simić, S., Topakas, E., & Nikodinovic-Runic, J. (2019). Applications of microbial laccases: Patent review of the past decade (2009–2019). *Catalysts*, 9(12), 1023. <https://www.mdpi.com/2073-4344/9/12/1023>. <https://doi.org/10.3390/catal9121023>
- Zheng, H., Chruszcz, M., Lasota, P., Lebioda, L., & Minor, W. (2008). Data mining of metal ion environments present in protein structures. *Journal of Inorganic Biochemistry*, 102(9), 1765–1776. <https://linkinghub.elsevier.com/retrieve/pii/S016201340800127X>. <https://doi.org/10.1016/j.jinorgbio.2008.05.006>